Applied Science and Innovative Research
ISSN 2474-4972 (Print) ISSN 2474-4980 (Online)
Vol. 8, No. 2, 2024
www.scholink.org/ojs/index.php/asir

*Original Paper*

# Research on AEB-P Control Strategy Considering Braking Process Comfort

Peng Yang[1*], Ying Lu[1] & Ye Chen[1]

[1] School of Automotive and Traffic Engineering, Jiangsu University, Zhenjiang, Jiangsu 212013, China

[*] Corresponding author, Peng Yang, E-mail: yangpeng037@163.com

Received: April 17, 2024 Accepted: May 3, 2024 Online Published: May 10, 2024

doi:10.22158/asir.v8n2p57 URL: http://doi.org/10.22158/asir.v8n2p57

***Abstract***

*A control approach for the pedestrian-oriented automobile automatic emergency braking system (AEB-P) that takes driving comfort into account is suggested in an effort to further optimize the AEB-P system's control algorithm. Firstly, for the AEB-P assessment standard of C-NCAP, a braking safety distance model that takes the driver's comfort into account during braking is created. The next step was to construct a hierarchical controller using PID and MPC principles. Lastly, CarSim and Matlab/Simulink are used to build and validate the test scenarios and control methods. The simulation results demonstrate that both ride comfort and driving safety can be guaranteed by the suggested control technique.*

***Keywords***

*vehicle engineering, automatic emergency braking, model predicative control, pedestrian collision avoidance*

## 1. Introduction

The World Health Organization estimates that 1.35 million individuals worldwide lose their lives in traffic accidents each year (World Health Organization, 2018), with vulnerable road users accounting for more than half of the fatalities. The number of pedestrian-vehicle collision (PVC)-related injuries and fatalities in China is rising annually (Tian, Zhang, & Wang, 2020). Therefore, the main goal of research on vehicle safety technologies is to determine how to prevent or minimize traffic safety mishaps. One significant automobile active safety technology that can significantly lower the death rate of VRUs in road accidents is autonomous emergency braking for pedestrians (AEB-P) (Fildes, Keall, Bos, Lie, Page, Pastor, Pennisi, Rizzi, Thomas, & Tingvall, 2015). As a result, numerous researchers have focused on enhancing and optimizing AEB-P performance. As research on AEB deepens, some academics have begun to design the brake recovery and release zones during partial braking and have begun to incorporate driver characteristics into the safety control strategy in an effort to prevent drivers from becoming so uncomfortable that they turn off the AEB-P system, which increases the safety hazard (Bae, Lee, & Kang, 2020).

This paper proposes an AEB-P safety distance algorithm that combines driving safety and comfort. Comfort is taken into consideration when designing a safety distance threshold model for the AEB-P evaluation standard of C-NCAP. In order to assess the efficacy of the approach presented in this paper and examine the experimental outcomes, an AEB-P test scenario is lastly constructed.

## 2. AEB-P Safety Assessment Modeling

### *2.1 Safe Distance Algorithm Considering Comfort*

In order to fully stop the car, the driver typically has to go through a number of phases, which are primarily broken down into the following stages: the stage of the driver's reaction ($0\sim t_1$); the stage of the driver touching the brake pedal control after finishing the reaction ($t_1\sim t_2$); the stage where the braking system coordinates the delay ($t_2\sim t_3$); the stage where the braking decelerates ($t_3\sim t_4$); the stage where the braking duration phase ($t_4\sim t_5$); and the stage where the braking ends ($t_5\sim t_6$). The duration of each stage of the braking process is shown by the $\Delta t_1$, $\Delta t_2$, $\Delta t_3$, $\Delta t_4$, $\Delta t_5$, $\Delta t_6$, respectively. Figure 1 depicts the change in brake deceleration during vehicle braking.

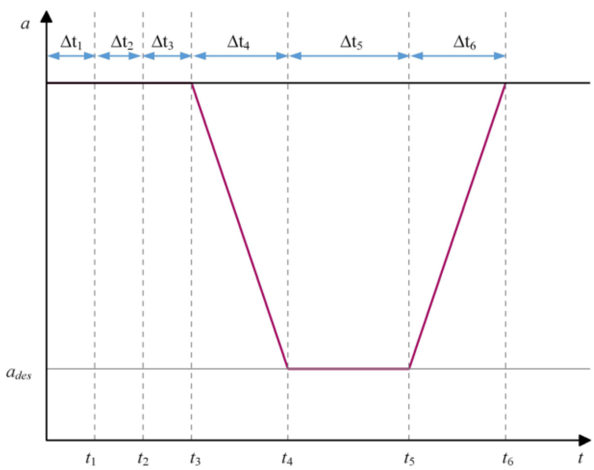


**Figure 1. Vehicle Braking Process**

The brake safety distance model is derived by examining the relationship between the relative velocity of pedestrians and self-vehicles, with an aim towards the typical AEB-P test scenarios specified by C-NCAP. When the active braking control is engaged, the AEB-P system's braking mechanism resembles that of the driver-controlled braking mechanism, except it lacks the $0\sim t_2$ phase.

Figure 1 illustrates how this paper introduces the rate of change of acceleration, which is computed as follows:

$$jerk(t) = \frac{a(t) - a(t - \triangle t)}{\triangle t} \tag{1}$$

Where, $jerk(t)$ is the acceleration change rate, $a(t)$ is the current acceleration, $a(t\text{-}\Delta t)$ is the acceleration of the previous moment , and $\Delta$t is the time interval between two acceleration signals. This study sets up a deceleration change buffer at the beginning and the end stages of braking respectively, so that the absolute values of $j_{\max}$ and $j_{\min}$ are equal.

Given that the buffer period in the configuration above is $\Delta t_4 = \Delta t_6$, the optimal vehicle brake deceleration following the activation of the AEB-P system is:

$$a_{des}(t) = \begin{cases} 0 & t \in (0, t_3) \\ jerk_{\min}(t - t_3) & t \in (t_3, t_4) \\ a_{d\max} & t \in (t_4, t_5) \\ a_{d\max} + jerk_{\max}(t - t_5) & t \in (t_5, t_6) \end{cases} \tag{2}$$

Where $a_{dmax}$ denotes the maximum braking deceleration, $t$ denotes the moment.

The car and pedestrian's longitudinal relative velocities are as follows:

$$v_{rel}(t) = v_2(t) - v_1(t) \tag{3}$$

Where the vehicle's velocity at time t is represented by $v_2(t)$, and the pedestrian's velocity at time t is represented by $v_1(t)$。

The optimum safe distance threshold can be determined as follows using figure 1 and the definition given above:

$$\begin{aligned} d_e &= (v_2 - v_1)\triangle t_3 + \int_{t_3}^{t_6} v_2(t) - v_1(t)\,dt + d_0 \\ &= (v_2 - v_1)t_h + d_0 \end{aligned} \tag{4}$$

Where, $v_2$ and $v_1$ are the speeds of vehicles and pedestrians before emergency braking, respectively, $t_h$ is the limit braking time threshold, $d_0$ indicates the minimum safe distance.

A study suggests that the AEB-P system shouldn't brake when the TTC is more than 2s in order to prevent interference with the driver's normal driving (Itoh, Inagaki, & Horikome, 2011). Consequently, this paper's technique specifies $t_{TTC}$ = 2s.

$$d_e = \begin{cases} (v_2 - v_1)t_h + d_0 & t_h \le t_{TTC} \\ (v_2 - v_1)t_{TTC} + d_0 & t_h > t_{TTC} \end{cases} \tag{5}$$

### *2.2 AEB-P Early Warning System*

The warning system is separated into three levels to increase driving safety and guarantee that the driver has enough reaction time. Level 1 indicates that the current driving safety, the early warning system sends out a signal value of 0 ($d_r > d_{wa}$). Level 2 signals that there is a possible collision risk due to the pedestrian in front of the vehicle and the driver's present driving condition ($d_{wa} \ge d_r \ge d_e$). The early warning system sends out a signal value of 1, and the AEB-P system reminds the driver by using sound and image signals. Level 3 indicates that the vehicle is headed for a collision with the pedestrian in front ($d_e \ge d_r \ge 0$), the early warning system will send out a signal value of 2, and if the driver hasn't engaged in self-braking or applied steering to avoid an obstacle. At this time, AEB-P will activate the brakes to avoid collision. Figure 2 depicts the early warning braking mode.

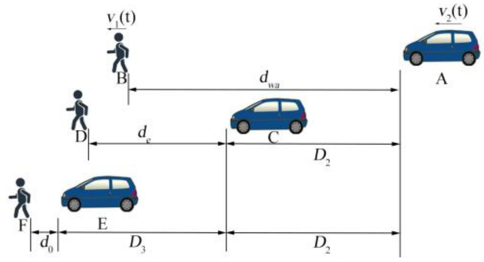


**Figure 2. Schematic Diagram of Pre-warning Braking Mode**

Therefore, the hazard descent distance threshold so as follows:

$$d_{wa} = d_e + v_{rel}\left(t\right)t_w \tag{6}$$

Where, $t_w$ is the driver reaction time. Statistically $t_w$ is usually 1.14s ~ 1.38 s (Coelingh, Eidehall, & Bengtsson, 2010), taking the average value of $t_w$ = 1.25 s.

## 3. MPC-based AEB-P Upper Control System

### 3.1 Longitudinal Dynamics Model

Human-vehicle longitudinal spacing, vehicle velocity, human-vehicle longitudinal relative velocity, vehicle acceleration, and rate of change of vehicle acceleration were chosen as state quantities of the control system, $\boldsymbol{x}(k)=[d_{\mathrm{rel}}(k), v_2(k), v_{\mathrm{rel}}(k), a_2(k), jerk(k)]^{\mathrm{T}}$, by analyzing the human-vehicle kinematics relationship. The equation of state model for longitudinal kinematics is constructed by choosing $\boldsymbol{y}(k)=[d_{\mathrm{rel}}(k), v_2(k), a_2(k)]^{\mathrm{T}}$ as the optimization target:

$$\begin{cases} \boldsymbol{x}\left(k+1\right) = \boldsymbol{A}_d\boldsymbol{x}\left(k\right) + \boldsymbol{B}_d u\left(k\right) \\ \boldsymbol{y}\left(k\right) = \boldsymbol{C}_d\boldsymbol{x}\left(k\right) \end{cases} \tag{7}$$

Where, $\boldsymbol{A}_d = \begin{bmatrix} 1 & 0 & -T_s & -\frac{1}{2}T_s^2 & 0 \\ 0 & 1 & 0 & T_s & 0 \\ 0 & 0 & 1 & T_s & 0 \\ 0 & 0 & 0 & 1-\frac{T_s}{\tau_d} & 0 \\ 0 & 0 & 0 & -\frac{1}{\tau_d} & 0 \end{bmatrix}$, $\boldsymbol{B}_d = \begin{bmatrix} 0 \\ 0 \\ 0 \\ \frac{T_s}{\tau_d} \\ \frac{1}{\tau_d} \end{bmatrix}$, $\boldsymbol{C}_d = \begin{bmatrix} 1 & 0 & 0 & 0 & 0 \\ 0 & 1 & 0 & 0 & 0 \\ 0 & 0 & 0 & 1 & 0 \end{bmatrix}$, $u(k)$ is the desired braking deceleration $a_{des}$, and $\tau_d$ is the 1st order inertial link time constant describing the transfer characteristics of the desired acceleration $u(k)$ and the actual acceleration $a_2(k)$ of the vehicle, $T_{\mathrm{s}}$ is the system sampling time.

### 3.2 AEB-P Performance Requirements and Constraints

The safety performance of the AEB-P system, which is its fundamental purpose, must be the most important evaluation index. The limitations between a human and a vehicle are as follows in order to provide safety and consider driving comfort at the same time:

$$\begin{cases} d_{rel} \geq d_0 \\ a_{d\max} \leq a(k) \leq a_{\max} \\ jerk_{\min} \leq jerk(k) \leq jerk_{\max} \\ u_{\min} \leq u(k) \leq u_{\max} \end{cases} \tag{8}$$

Where, $a_{d\max}$ and $a_{\max}$ denote the minimum and maximum values of the acceleration of the vehicle, respectively, respectively.

In contrast to AEB, AEB-P should stop as soon as it is safe to do so and stop the car at zero speed to protect pedestrians. The optimization objective is stated below:

$$\begin{cases} v_2(k) \to 0 \\ d_{rel} \to d_0 \\ \min\left|a_2(k)\right| \end{cases} \tag{9}$$

*3.3 MPC Controller Solving*

According to equation (7), the prediction equation in the prediction time domain can be established, defining $\boldsymbol{e}(k)$ as the error between the actual state quantity and the predicted value, and the following model can be established:

$$\begin{cases} \boldsymbol{X} = \boldsymbol{A}_p \boldsymbol{x}(k) + \boldsymbol{B}_p \boldsymbol{U}(k) + \boldsymbol{F}_p \boldsymbol{e}(k) \\ \boldsymbol{Y} = \boldsymbol{C}_p \boldsymbol{x}(k) + \boldsymbol{D}_p \boldsymbol{U}(k) + \boldsymbol{H}_p \boldsymbol{e}(k) \end{cases} \tag{10}$$

Where, $\boldsymbol{X}$ is the ensemble of predicted state variables in the prediction time domain $N_p$, $\boldsymbol{Y}$ is the predicted output variables in the prediction time domain $N_p$, and $\boldsymbol{U}(\boldsymbol{k})$ is the sequence of expected acceleration output variables in the control time domain $N_c$, which are involved in the prediction model for each prediction matrix $\boldsymbol{A_p}$, $\boldsymbol{B_p}$, $\boldsymbol{F_p}$, $\boldsymbol{C_p}$, $\boldsymbol{D_p}$, $\boldsymbol{H_p}$.

The objective function of the integrated analytical design optimization for the control performance requirements of the AEB-P system is defined as:

$$J_r = \sum_{i=1}^{N_p} \left\| \boldsymbol{y}_p(k+i|k) - \boldsymbol{y}_{ref}(k+i|k) \right\|_{\boldsymbol{Q}}^2 + \sum_{i=1}^{N_c} \left\| u(k+i) \right\|_{\boldsymbol{R}}^2 + \rho\varepsilon^2 \tag{11}$$

Where, $\boldsymbol{y}_p(k+i|k)$ is the predicted value of the system at moment k for the control output quantity at moment k+i, $\boldsymbol{y}_{ref}(k+i|k)$ denotes the reference value corresponding to the control output, $u(k+i)$ is the control input at moment k+i, $\boldsymbol{Q}$ is the matrix of the output quantity weight coefficients, $\boldsymbol{R}$ is the incremental weight matrix of the control quantity, $\varepsilon$ and $\rho$ are the relaxation factor and the corresponding weight coefficients.

Using the quadprog function of the Matlab optimization toolbox, we convert equation (12) into a typical quadratic programming problem and solve it. The result is a list of optimal control quantities in the control time domain that correspond to each sampling moment:

$$\boldsymbol{U}^*(k)=\left[u^*(k),u^*(k+1)\cdots,u^*(k+N_c-1)\right]^T \tag{13}$$

## 4. Lower PID Control System and Vehicle Model

### *4.1 Lower Controller Design*

The main function of the lower controller of the AEB-P is to control and execute the above vehicle dynamics model, and to perform real-time control by accepting the upper control signal and converting the brake pressure value. Due to the nonlinear characteristics of the longitudinal dynamics of the vehicle, there is an error between the actual acceleration of the vehicle and the desired value, and the acceleration error is controlled by using the PID control strategy, which takes the difference between the desired state and the actual state output from the upper layer MPC controller as the control error $e(t)$, as:

$$e(t)=a_2(t)-a_{des}(t) \tag{14}$$

Where, $a_2(t)$ is the actual self-vehicle acceleration, and $a_{des}(t)$ is the desired acceleration of the self-vehicle.

The lower layer control law is expressed as:

$$p_b(t)=K_p\left[e(t)+\frac{1}{T_i}\int_0^t e(t)dt+T_d\frac{de(t)}{dt}\right] \tag{15}$$

Where, $K_P$, $T_i$ and $T_d$ are the proportional gain, integral time constant and differential time constant of the PID controller, $p_b(t)$ is the output braking pressure value. The three control parameters of the PID controller are set as: $K_P = 3$, $T_i = 15$ and $T_d = 0.01$.

### *4.2 Vehicle Modeling*

We took a certain C-class car as the research object and established an accurate vehicle dynamics model by Carsim software. The main parameters of the whole vehicle are shown in Table 1 below.

**Table 1. Main Parameters of the vehicle**

| Parameter | Value | Unit |
|---|---|---|
| Vehicle curb quality | 1270 | kg |
| Engine rated power | 125 | kW |
| Air resistance coefficient | 0.3 | - |
| Frontal area | 2.3 | $m^2$ |
| Rolling friction coefficient Wheelbase | 2.656 | m |
| The center of gravity to the center of the front wheel | 1. 615 | m |
| Rolling friction coefficient | 0.025 | - |
| Tire rolling radius | 0.345 | m |
| Ratio of braking torque to braking pressure at the front wheels | 240 | N m/Mpa |
| Ratio of braking torque to braking pressure at the rear wheels | 110 | N m/Mpa |

**5. AEB-P System Validation and Analysis**

In order to verify the effectiveness of the designed AEB-P control strategy, this paper refers to the classic AEB-P test scenarios in the China New Car Assessment Program (C-NCAP), and uses the Carsim software to establish the scenario in which the most likely human-vehicle collision accidents occur in the Car-to-Pedestrian Longitudinal Adult (CPLA), and establishes the control strategy of the present study, the traditional control strategy, and the vehicle control model in Simulink. In this paper, the hardware-in-loop (HiL) test is used to verify the simulation, such as Figure 3 shows the general scheme of the test.

In order to test the performance of the designed AEB-P strategy (Strategy 1) under different working conditions, there are five sets of test conditions, the test scenario is CPLA-50, Vehicle speed range 20-60 km/h in 10 km/h steps, and comparing it with the AEB-P strategy (Strategy 2) that adopts a fixed TTC threshold, which is set to 1.0 s, and the braking delay time is 0.2 s. The CPLA-50 means that the vehicle will collide with a pedestrian without any braking or steering being applied and the point of collision is at 50% of the vehicle width. The pedestrian speed in the CPLA scenario was 5 km/h longitudinally.

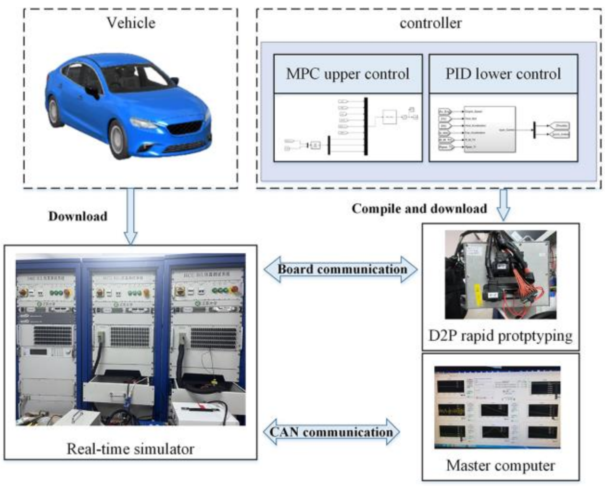


**Figure 3. General Scheme for Hardware-in-loop Testing**

When the vehicle speed is 60 km/h, the braking process of CPLA-50 condition is shown in Figure 4. In Figure 4, the AEB-P control strategy in this paper triggers the braking strategy at approximately 1.7 s, and the braking acceleration reaches the maximum after 0.8 s. The traditional AEB-P control strategy triggers the braking strategy at about 2.3 s, and the braking acceleration reaches the maximum after 0.1 s. However, due to the late braking trigger timing, it fails to avoid the collision with the pedestrian in front of it.

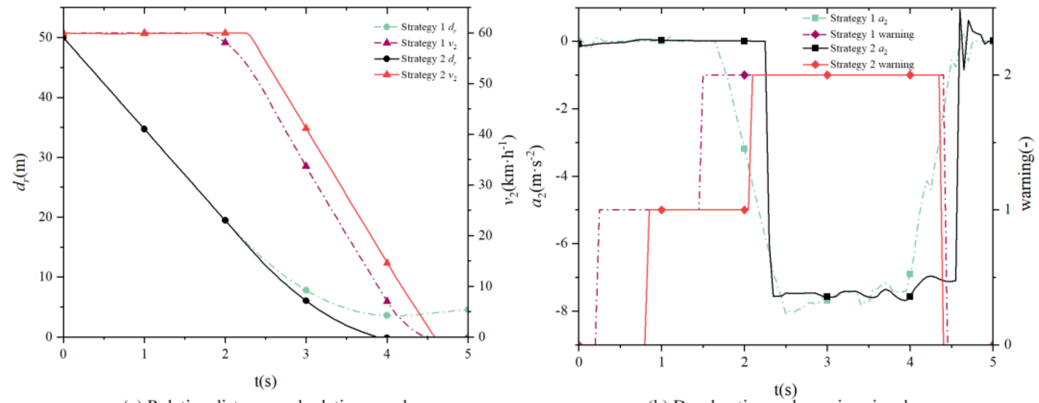


(a) Relative distance and relative speed (b) Deceleration and warning signals

**Figure 4. CPLA-50 Scene Braking Process**

The pedestrian speed in the CPLA scenario was 5 km/h longitudinally, and the test vehicles traveled uniformly forward at different speeds. The specific test results under the CPLA-50 scenario are shown in Table 2 below. Combined with Table 2, we can analyze the test results: under the AEB-P control strategy in this paper, the maximum braking acceleration is controlled at -6.18 m s$^{-2}$ ~ -8.09 m s$^{-2}$, and the minimum longitudinal distance between the vehicle and the pedestrian in the successful collision avoidance scenario is maintained at 2.58 m ~ 3.54 m, which is capable of avoiding some unnecessary injuries. Under the traditional control strategy, the minimum longitudinal distance between the vehicle and the pedestrian in the successful collision avoidance situation is kept at 2.18 m ~ 5.13 m, and the maximum braking acceleration range is 7.60 m s$^{-2}$ ~ 7.75 m s$^{-2}$, which can not avoid the collision when the vehicle travels at a speed of more than 60 km/h.

**Table 2. Simulation Results of CPLA-50 Scene**

| Speed | Minimum spacing during braking $d_r$ (m) | | Relative velocity of collision (km h$^{-1}$) | | $a_{d\max}$ |
|---|---|---|---|---|---|
| (km h$^{-1}$) | Strategy 1 | Strategy 2 | Strategy 1 | Strategy 2 | /m s$^{-2}$ |
| 20 | 2.58 | 5.13 | - | - | -6.18 |
| 30 | 2.61 | 5.17 | - | - | -6.53 |
| 40 | 2.61 | 4.23 | - | - | -7.17 |
| 50 | 2.86 | 2.18 | - | - | -7.52 |
| 60 | 3.54 | - | - | 12.34 | -8.09 |

## 6. Conclusions

This work proposes an adaptive AEB-P system control algorithm that takes ride comfort and driving safety into account during the braking phase.

In contrast to the conventional fixed TTC threshold algorithm, the control algorithm presented in this paper performs better overall. It not only increases safety but also modifies the braking deceleration more gradually throughout the braking process. This work presents a strategy that, to some extent, accounts for driving comfort while avoiding the discomfort induced by the abrupt shift in braking deceleration when AEB-P intervenes and withdraws from braking under safety conditions. When compared to the conventional control strategy, this paper's method can help the autonomous vehicle and the pedestrian in front of it maintain a more stable minimum distance, and its robustness is better, in the event that both the traditional method and this one are successful in preventing collisions.

The test scenarios in this study only take into account driving situations on flat and straight roads. These driving scenarios are somewhat basic, and the next stage will be to think about building the control algorithms under more complicated test scenarios, including curves.

**Funding**

This work was supported by the National Natural Science Foundation of China (No. 51605197); the Key Research and Development Plan of Zhenjiang City (No. SH2019054).

**References**

Bae, J.-J., Lee, M.-S., & Kang, N. (2020). Partial and Full Braking Algorithm According to Time-to-Collision for Both Safety and Ride Comfort in an Autonomous Vehicle. *Int. J. Automot. Technol.*, *21*(2), 351-360. https://doi.org/10.1007/s12239-020-0033-8

Coelingh, E., Eidehall, A., & Bengtsson, M. (2010). Collision Warning with Full Auto Brake and Pedestrian Detection - a Practical Example of Automatic Emergency Braking. In *13th International IEEE Conference on Intelligent Transportation Systems*, pp. 155-160. https://doi.org/10.1109/ITSC.2010.5625077

Fildes, B., Keall, M., Bos, N., Lie, A., Page, Y., Pastor, C., Pennisi, L., Rizzi, M., Thomas, P., & Tingvall, C. (2015). Effectiveness of Low Speed Autonomous Emergency Braking in Real-World Rear-End Crashes. *Accid. Anal. Prev.*, *81*, 24-29. https://doi.org/10.1016/j.aap.2015.03.029

Itoh, M., Inagaki, T., & Horikome, T. (2011). Design and Evaluation of Situation-Adaptive Pedestrian-Vehicle Collision Avoidance System. In *2011 IEEE International Conference on Systems, Man, and Cybernetics*, pp. 1063-1068. https://doi.org/10.1109/ICSMC.2011.6083815

Tian, J., Zhang, C., & Wang, Q. (2020). Analysis of Craniocerebral Injury in Facial Collision Accidents. *PLoS ONE*, *15*(10), e0240359. https://doi.org/10.1371/journal.pone.0240359

World Health Organization. (2018). Global Status Report on Road Safety 2018: Summary. *World Health Organization*, 2018.